

Enviro. Treat. Tech. ISSN: 2309-1185

Journal web link: http://www.jett.dormaj.com



Geophysical Exploration Studies of Additional Structures of Phase 12 of South Pars Gas (Tombak Region)

Alireza Ashofteh and Sharareh Haj Ali

Young Researchers and Elite Club, Islamic Azad University North Tehran Branch, Tehran, Iran, St_a_ashofteh@azad.ac.ir Master of Geology Tectonics, Islamic Azad University North Tehran Branch, Tehran, Iran, Sh.Ha_7@yahoo.com

Abstract

South pars gas complex, phase 12 is located in south of Iran, about 17km east of Kangan, Busheher province. In this study 6 seismic refraction profiles with refraction method have been taken. Down-hole seismic profiles have been taken in 4 drilled boreholes (down-hole) for determining P-wave and S-wave velocity and 22 electrical resistivity sounding have been taken for determining geological condition of layers. Also points with Schulmberger-Weener array have been taken.

Key words: Geophysical Exploration, South Pars Gas, Structure, Tombak.

1 Introduction

The location map of study area is shown in Fig (1). The satellite picture of the site is presented in Fig (2). The plan of project which is reclamation from the sea by filling sea with soil and rock is shown in Fig (3). Also, some pictures of site location are presented in Fig (4). In this study 6 seismic refraction profiles of P-waves and S-wave velocity, 4 Down-hole seismic profiles of P-wave and S-wave velocity and 22 electrical resistivity sounding points with Schulmberger-Weener array have been taken. The location map of seismic profiles, drilled boreholes and electrical resistivity sounding point has been shown in Fig (2).

2 Investigation procedures

Identifying subsurface layers condition and its dynamic properties are main factors in dynamic analysis of construction. In order to completing geotechnical information, seismic testes included refraction and Downhole has been done. In this study 6 refraction seismic profiles of P-wave and S-wave and 4 Down-hole seismic profiles of P-wave and S-wave have been taken. For this study following equipment have been used:

- (1) Seismograph RAS 24.
- (2) 3-Component borehole geophone.
- (3) 6-Geophone borehole streamer (Spacing 2m).
- (4) Vertical geophones.
- (5) Horizontal geophones.
- (6) Hammer.
- (7) Wooden plank.
- (8) Battery (12volt DC).
- (9) Global Positioning System (GPS).
- (10) Notebook computer.
- (11) Other accessory, cable, reel, wire and etc.



Fig. 1: Vicinity of the project site



Fig. 2: Site location on the satellite photo

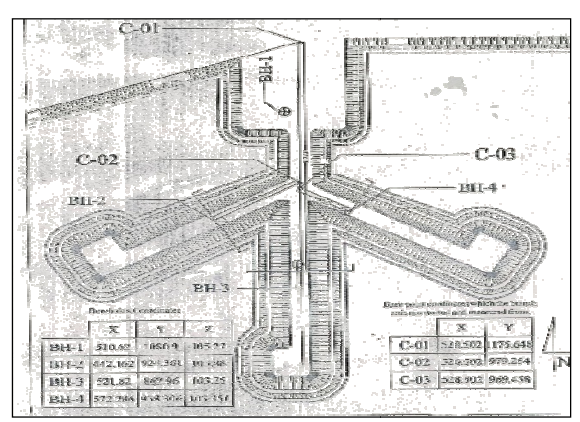


Fig. 3: Site plan and location of drilled boreholes



Fig. 4: Prepared ground in the sea for offshore structures location

3 Theory of Seismic Tests

Geophysical explorations are used to study tectonics characteristic and geology, identified geology layering, estimate of dynamic properties of materials, considering of behaviour of soil under earthquake. Geophysical method divided into two groups. In the first group the physical quality natural source is considering. This group included gravity, magnetic, radiometry and thermometry and seism city. The second group included the method that measuring response of non-natural or synthetic source. In this group can called seismic refraction, reflection, geoelectric, induced polarization and electromagnetic. Seismic methods are included refraction, reflection, down hole, cross hole, and tomography cross hole. Here we present the theory of seismic, refraction and down hole methods. These methods are commonly used to determine compression and shear wave velocity versus depth. These velocity data are used to help assess the seismic response and determine stratigraphy of a particular site. In a down hole seismic survey a seismic source is placed on the surface near a borehole and a geophone is placed at selected depths in the borehole. The raw data obtained from a down hole survey are the travel times for compression and shear waves from the source to the geophones and the distance between the source and geophones. Compression waves are generated by striking a sledge hammer on steel plate. The steel plate is located at short distance from the boring mouth. Shear waves travel slower than compression waves. Therefore, compression waves often interfere with shear waves. This interference sometimes makes identification of the first shear wave arrival difficult. To improve the resolution of the shear wave arrival the seismic source is designed to produce a signal which contains a large shear wave component and a signal enhancement seismograph is used to process the received signals from the geophone. The shear wave source consists of sledge hammer impacts on alternate ends of a beam with steel end plates. The beam is offset a distance of five to ten feet from the borehole to minimize direct coupling of the seismic energy to the casing.

A. Refraction method

Seismic refraction surveying is the first major geophysical method to be applied in the search for oil bearing structures. Recent progress in geophysical exploration from computer assisted processing and enhancement of the data can assist in resolving complicated problems in structural geology and engineering. Refraction is a usual method in engineering geophysical exploration. Low cost, simple in survey and varity in interpretation of this method caused it uses more and more in study of site in different engineer size. The refraction method consists of measuring the first travel times of compression or shear waves generated by an impulsive energy source. The energy source is usually a small explosive charge or strike hammer. The arrivals of different kinds of seismic waves are detected by geophones array and recorded by seismograph. By extracting time distance curves from seismograms we can calculate seismic parameters of section such as wave velocities and thicknesses of lavers. The process is schematically illustrated in Fig(1-1). All measurements are made at surface of the ground and the subsurface structure is inferred from interpretation methods based on the law of energy propagation. The propagation of seismic energy through subsurface layers is described by essentially the same rules that govern the propagation of light rays through transparent media. The refraction or angular deviation that a light ray or seismic pulse undergoes when passing from one material to another depends upon the ratio of the transmission velocities of the two materials. The fundamental law that describes the refraction of light ray is Snell's law and this together with the phenomenon of "critical incidence" is the physical foundation of seismic refraction surveys. Suppose a medium with a velocity V_1 underline a medium with a

higher velocity V_2 ($V_2 > V_1$). Until the critical angle of incidence is reached almost all of the compression energy is transmitted(refracted) into the higher velocity medium when the critical angle is exceeded the energy is almost totally reflected and no energy is refract into the high speed layer in the refraction equations assume that the subsurface layers possess certain characteristics: each layer within a stratigraphic sequence is isotropic with regard to its proportion velocity ray paths water supply are made up of straight line segment and each layer has a higher velocity than overlying one. These are entirely reasonable assumptions and relatively few actual cases will depart from these assumptions. In this method produce the seismic

wave by synthetic energetically source(explosion, sparker or hammer) at a point and received by array of receivers in a straight line. With releasing energy to distance from source called cross over distance the first wave received directly that has velocity V_{l} and travel time has following

equation: $t_1 = X/V_1$

 t_1 : Direct travel time

X: Distance between source and receiver

V₁: Velocity in surface layer

After this distance waves refract in second layer with velocity of sub layer. Equation between time and distance for a model included two horizontal layers as follow:

$$t_{2} = \frac{X}{V_{2}} + \frac{2H_{1}Cos\theta}{V_{1}} \hspace{1cm} ; \hspace{0.5cm} V_{2} > V_{1}$$

H1: Thickness of first layer

 V_1 , V_2 : Velocity in first layer and second layer

 θ : Critical angle

t2: Received time of refracted wave

With plotting of travel time verse distance the velocity of first layer obtained from inverse of slope in first medium and the second layer from inverse of slope in second medium.

B. Down-hole method

This method is commonly used to determine compression and shear wave velocity versus depth. These velocity data are used to help assess the seismic response and determine stratigraphy of a particular site. In a down hole seismic survey, a seismic source is placed on the surface near a borehole and two geophones are placed at selected depths in the borehole. The raw data obtained from a down hole survey are the travel times for compression and shear waves from the source to the geophones and the distance between the source and geophones. The process is schematically illustrated in Fig (1-2). Compression waves are generated by striking a sledge hammer on steel plate. The steel plate is located at short distance from the boring mouth. Shear waves travel slower than compression waves. Therefore, compression waves often interfere with shear waves. This interference sometimes makes identification of the first shear wave arrival difficult. To improve the resolution of the shear wave arrival the seismic source is designed to produce a signal which contains a large shear wave component and a signal enhancement seismograph is used to process the received signals from the geophone. The shear wave source consists of sledge hammer impacts on alternate ends of a wooden beam with steel end plates. The beam is coupled to the ground by weighing it down with the front tires of the field recording truck. The beam is offset a distance of five to ten feet from the borehole to minimize direct coupling of the seismic energy to the casing. The down hole sensors consist of a three component geophone. This assembly contains three sensor elements

one vertical and two orthogonal horizontal elements. The geophone assemblies at a fixed separation are used so that interval velocities can be determined from the same set of impulses. This method reduces timing errors caused by differences in seismic triggering and variations in source impulse characteristics. The data are analyzed by determining the interval velocity for each geophone placement. Interval velocity is determined by first computing the distance from the source to each geophone and the difference in arrival times between the upper and lower geophones. The interval velocity is computed by dividing the difference in distance between the geophones by the difference in arrival times.

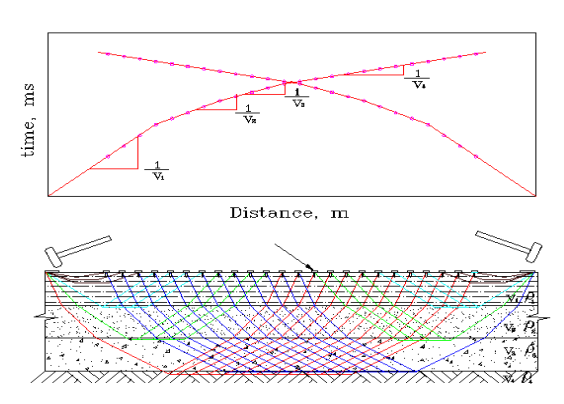


Fig (1-1): Schematic of ray path and time distance curves in refraction method

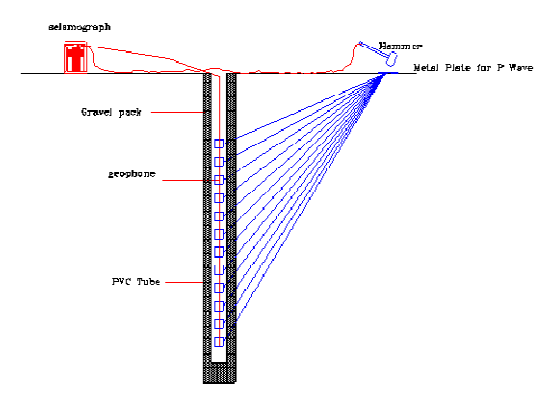


Fig (1-2): Schematic of Down hole test

4 Values of Velocity and Dynamic Property of Different Materials

Dynamic properties of materials are important in most projects. These parameters obtained either from dynamic and cyclic tests in geotechnical laboratory or geophysical tests. Longitudinal and shear wave velocity are measured by geophysical test and density is measured for by geotechnical test. For example the longitudinal and shear wave velocity of some type materials are bring in Table(1-1). Relationship between dynamic properties of solid and liquid are presented in Table(1-2). In this table V_p is

longitudinal velocity, V_s is shear velocity and d is density. The main parameter in geotechnical and civil engineering is shear modulus.

Table (1-1): Longitudinal, shear velocity and density of

	different materials					
Type of material	Density (gr/cm3)	Vp (m/s)	Vs (m/s)			
Water	1.0	1500	_ ` ′			
Sand & Gravel	1.5 - 2.0	500 - 1900	300 - 900			
Silt & Clay	1.3 - 1.7	300 - 1900	100 - 500			
Marl	1.3 - 1.7	300 - 1900	100 - 500			
Gypsum	1.8 - 2.2	1700 - 3000	600 - 1500			
Stiff Limestone	2.5 - 2.7	3000 - 6500	1500 - 3500			
Weathered Granite	2.0 - 2.7	1000 - 3000	500 - 1500			
Intact Granite	2.6 - 2.8	3000 - 6000	1500 - 3000			
Slate Rock	2.7	5000 - 7000	3000 - 3800			

Table (1-2). Relationship between dynamic modulus and longitudinal and shear wave velocity

31101	studinar and shour wave v	ciocity
Dynamic Parameters	Solids	Fluids
Poisson's ratio	$v = \frac{(\frac{V_p}{V_s})^2 - 2}{2[(\frac{V_p}{V_s})^2 - 1]}$	0.5
Wave velocity ratio	$(\frac{V_{p}}{V_{s}})^{2} = \frac{2 - 2v}{1 - 2v}$	∞
Shear modules	$G = \rho . V_s^2$	0
Yung modules	E = 2G(1+v)	0
Balk modules	$K = \frac{1}{3} \cdot \frac{E}{1 - 2\nu}$	$ ho V_p^2$

5 Refraction Seismic Results

For determining P-wave velocity, twelve vertical geophones with spacing 4m have been instaled in one line. Then by stricken hammer on metal plate at 4 location(4 and 13m offset from first and last geophone) seismic wave have been recorded. For determining S-wave velocity, twelve horizontal geophones with spacing 4m have been planted in one line. Then by stricken hammer horizontally on two side of wooden plank at 4 location (4 and 13m offset from first and last geophone) seismic wave have been recorded. The location map of refraction seismic profiles are presented in Fig (1-3). Also two sample of P-wave seismograph are shown in Figs (1-4) and (1-5). Seismic data with software has been interpreted and then results have been presented as profile.

5.1 Refraction profile p1

This profile has been taken entrance of site. P-wave and S-wave is velocity sections are shown sequence in Figs (1-6) and (1-7). With increasing depth density and velocity increased. P-wave velocity at Z=101m increases due to water velocity. In this profile shear wave velocity is variable from 450 to 700m/sec.

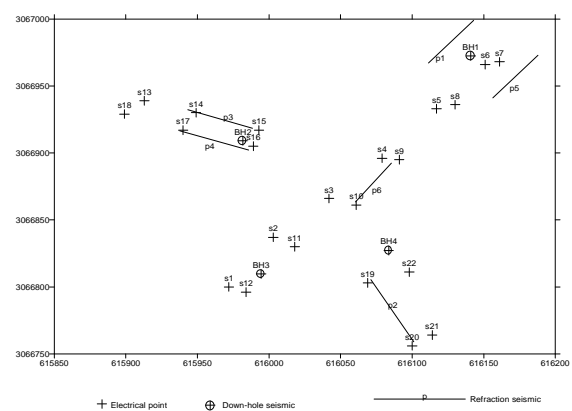


Fig (1-3): Location map of refraction seismic profiles

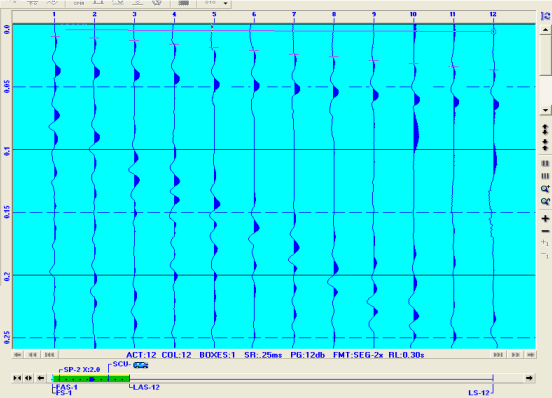


Fig (1-4): A seismograph of P-wave, offset 4m from first geophone

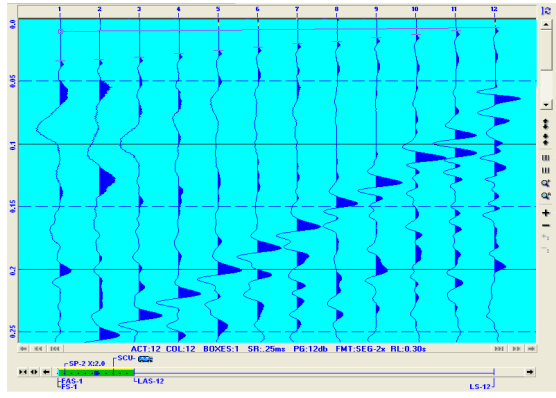


Fig (1-5): A seismograph of P-wave, offset 4m from last geophone

5.2 Refraction profile p2

This profile has been taken on east branch of site. P-wave and S-wave is velocity sections are shown sequence in Figs (1-8) and (1-9). With increasing depth density and velocity increased. P-wave velocity at Z=101.5m increases due to water velocity. In this profile shear wave velocity is variable from 450 to 700m/sec.

5.3 Refraction profile p3

This profile has been taken on west branch of site. Pwave and S-wave is velocity sections are shown sequence in Figs (1-10) and (1-11). With increasing depth density and velocity increased. P-wave velocity at Z=102m increases due to water velocity. In this profile shear wave velocity is variable from 450 to 700m/sec.

5.4 Refraction profile p4

This profile has been taken on west branch of site. P-wave and S-wave is velocity sections are shown sequence in Figs (1-12) and (1-13). With increasing depth density and velocity increased. P-wave velocity at Z=102m increases due to water velocity. In this profile shear wave velocity is variable from 400 to 700m/sec.

5.5 Refraction profile p5

This profile has been taken on main branch of site. P-wave and S-wave is velocity sections are shown sequence in Figs (1-14) and (1-15). With increasing depth density and velocity increased. P-wave velocity at Z=102m increases due to water velocity. In this profile shear wave velocity is variable from 400 to 700m/sec.

5.6 Refraction profile p6

This profile has been taken on main branch of site. P-wave and S-wave is velocity sections are shown sequence in Figs (1-16) and (1-17). With increasing depth density and velocity increased. P-wave velocity at Z=102m increases due to water velocity. In this profile shear wave velocity is variable from 450 to 730m/sec.

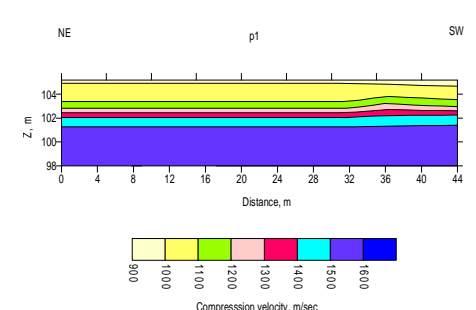


Fig (1-6): Iso velocity of compression velocity section in refraction seismic profile p1

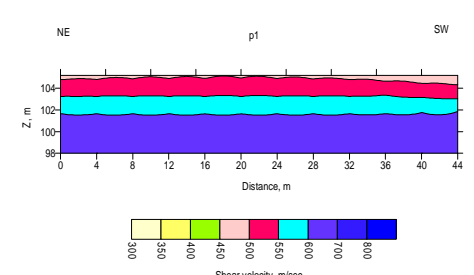


Fig (1-7). Iso velocity of shear velocity section in refraction seismic profile p1

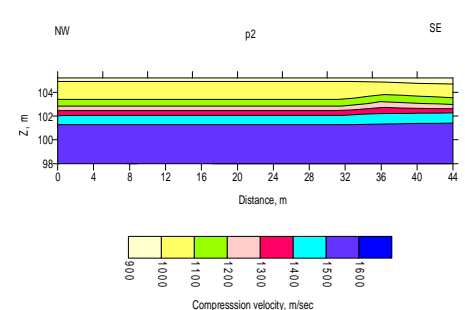


Fig (1-8): Iso velocity of compression velocity section in refraction seismic profile p2

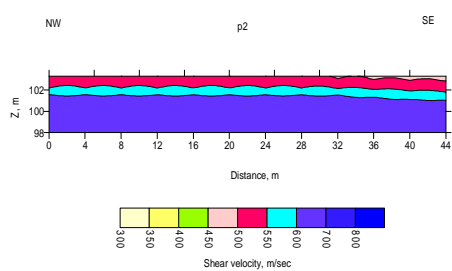


Fig (1-9): Iso velocity of shear velocity section in refraction seismic profile p2

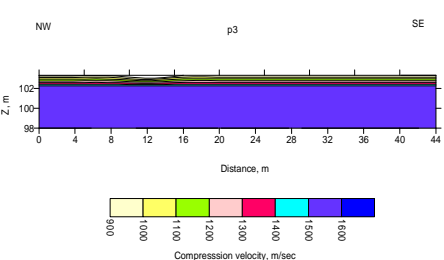


Fig (1-10): Iso velocity of compression velocity section in refraction seismic profile p3

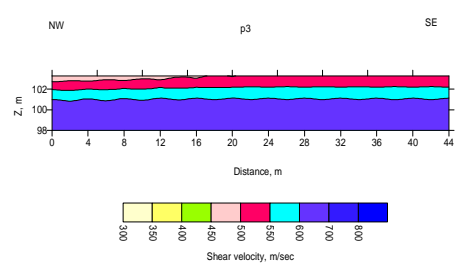


Fig (1-11): Iso velocity of shear velocity section in refraction seismic profile p3

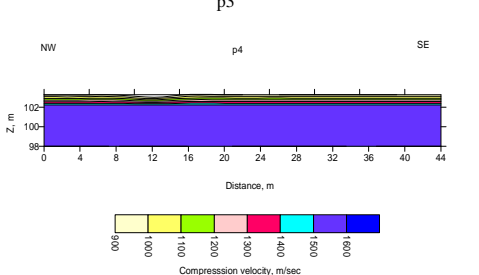


Fig (1-12): Iso velocity of compression velocity section in refraction seismic profile p4

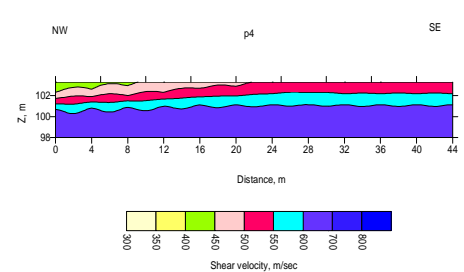


Fig (1-13): Iso velocity of shear velocity section in refraction seismic profile p4

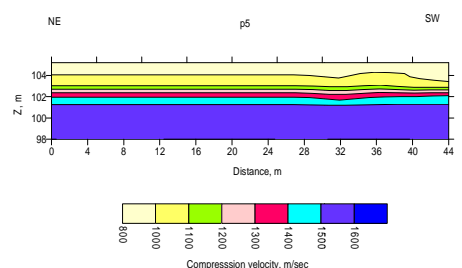


Fig (1-14): Iso velocity of compression velocity section in refraction seismic profile p5

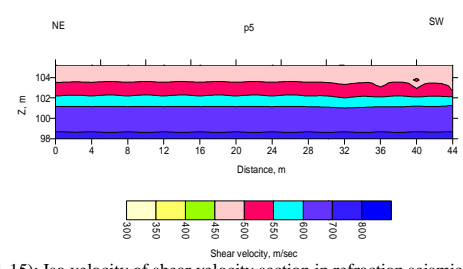
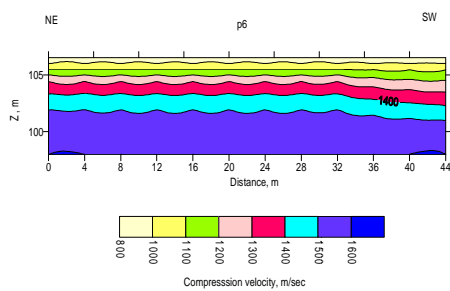


Fig (1-15): Iso velocity of shear velocity section in refraction seismic profile p5



Fig(1-16). Iso velocity of compression velocity section in refraction seismic profile p6

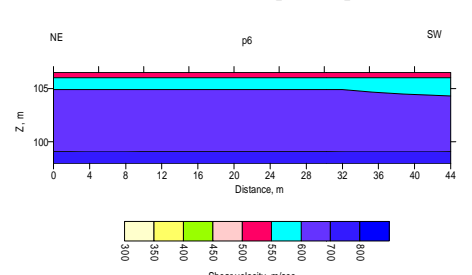


Fig (1-17): Iso velocity of shear velocity section in refraction seismic profile p6

5. Results of Down Hole Tests

Seismic study with down hole method in 4 boreholes BH-1, BH-2, BH-3 and BH-4 has been done. For determining of compression velocity, seismic source(vertical strike hammer on plate) located about 2.5m from mouth of borehole and receiver(3-componenet) swept all of depth borehole. For determining of shear velocity, seismic source(horizontal strike hammer on side of wooden plank) located about 3.0m from mouth of borehole and receiver(3-componenet) swept all of depth borehole. Local coordinates of drilled borehole are presented in Table(1-3). In Figs(1-18) and (1-19) sample seismograph of compression and shear wave have been shown.

Table (1-3): Coordinate of drilled boreholes that down hole seismic test have been done

seisine test have been done				
Borehole	X	Y		
BH-1	616141.6	3066972.0		
BH-2	615981.6	3066909.0		
BH-3	615994.5	3066809.6		
BH-4	616083.6	3066827.1		
	Borehole BH-1 BH-2 BH-3	BH-1 616141.6 BH-2 615981.6 BH-3 615994.5		

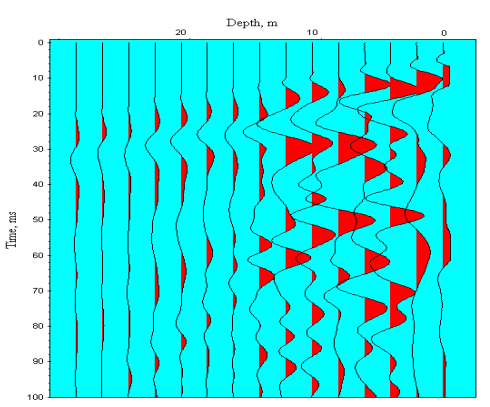


Fig (1-18): A sample of recorded compression wave seismograph in BH-1

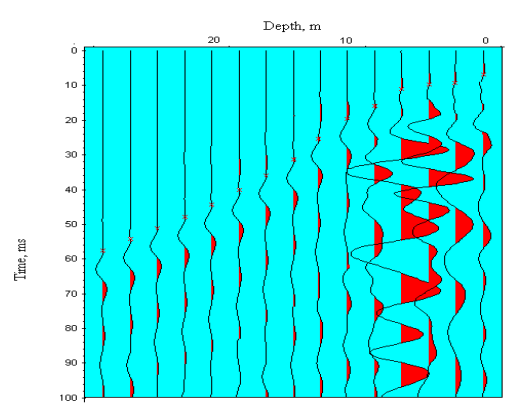


Fig (1-19): A sample of recorded shear wave seismograph in BH-1 $\,$

6.1 Down hole test in BH-1

Test characteristic of compression and shear wave velocity have been obtained by down hole seismic test in BH-1 are shown in Table(1-4) and Fig(1-20). Based on changing seismic velocity some layers physically can be distinguished. From 0 to 7m there is man-made soil such as

cobble, boulder and gravel. From 7 to end of borehole there is seabed materials such as sand, silt, loam shell and gravel that with increasing depth increasing density and velocity. Depth of groundwater during test is about 3.5m. In Table(1-4) Compression velocity(Vp), Shear velocity(Vs), Elastic modulus(E), Shear modulus(G), Bulk modulus(K) and Possion ratio(v) are presented.

Table (1-4): Characteristic of compression and shear wave velocity accompany with dynamic parameters in BH-1

Depth(m)	Density(gr/cm3)	Vp(m/sec)	Vs(m/sec)	E(MPa)	G(MPa)	K(MPa)	v
0-1	2	980	550	1537	605	1114	0.27
1-2	2	1050	600	1811	720	1245	0.26
2-3.5	2	1100	640	2038	819	1328	0.24
3.5-5	2	1500	650	2340	845	3373	0.38
5-7	2	1550	700	2689	980	3498	0.37
7-10	1.8	1600	350	650	221	4314	0.47
10-17	1.85	1600	400	868	296	4341	0.47
17-24	1.9	1600	520	1481	514	4179	0.44
24-28	2	1600	600	2042	720	4160	0.42

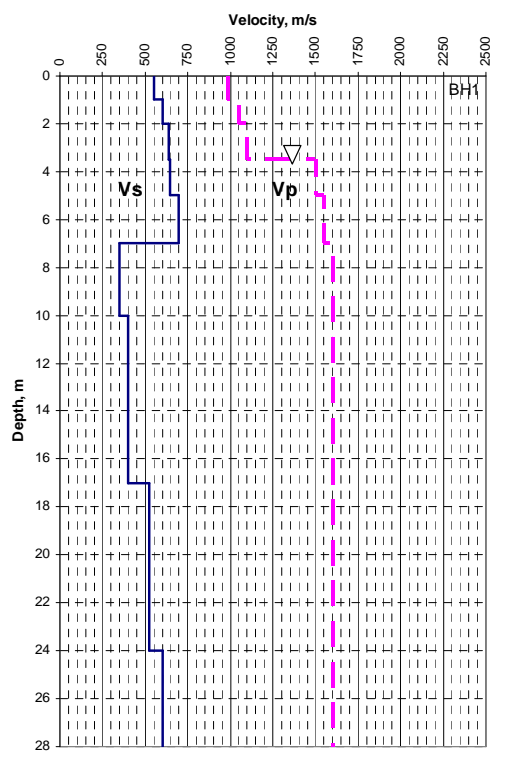


Fig (1-20): The variation of compression and shear velocity verse depth in $$\operatorname{BH-1}$$

6.2 Down hole test in BH-2

Characteristic of compression and shear wave velocity have been obtained by down hole seismic test in BH-2 are shown in Table (1-5) and Fig (1-21). Based on changing seismic velocity some layers physically can be distinguished. From 0 to 7m there is filler material such as cobble, boulder and gravel. From 7 to end of borehole there is seabed materials such as sand, silt, loam shell and gravel that with increasing depth increasing density and velocity. Depth of water during test is about 3.5m. In Table(1-5) Compression velocity(Vp), Shear velocity(Vs), Elastic

modulus(E), Shear modulus(G), Bulk modulus(K) and Poisson ratio(v) are presented.

Table (1-5): Characteristic of compression and shear wave velocity accompany with dynamic parameters in BH-2

Depth(m)	Density(gr/cm3)	Vp(m/sec)	Vs(m/sec)	E(MPa)	G(MPa)	K(MPa)	v
0-1	2	850	480	1167	461	831	0.27
1-2	2	1000	570	1637	650	1134	0.26
2-3	2	1500	630	2211	794	3442	0.39
3-5	2	1550	650	2355	845	3678	0.39
5-6	2	1600	700	2708	980	3813	0.38
6-7	1.85	1500	500	1330	463	3546	0.44
7-12	1.9	1550	400	890	304	4159	0.46
12-17	1.95	1600	450	1151	395	4466	0.46
17-20	2	1600	500	1446	500	4453	0.45

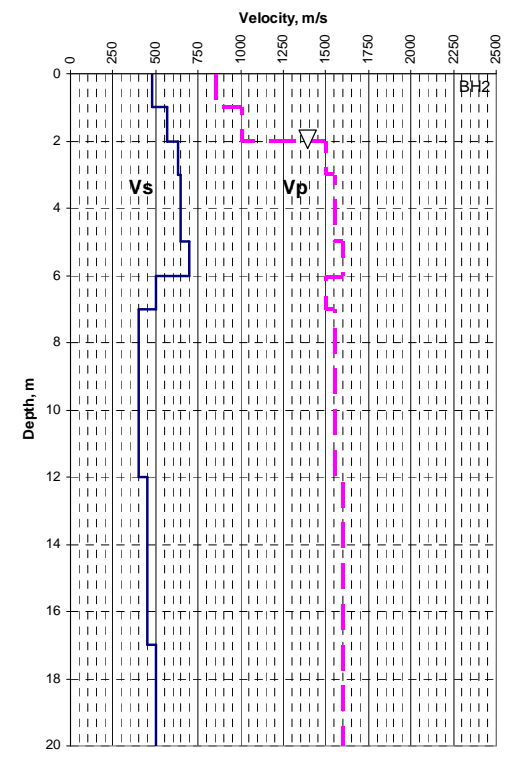


Fig (1-21): The variation of compression and shear velocity verse depth in $$\operatorname{BH-2}$$

6.3 Down hole test in BH-3

Characteristic of compression and shear wave velocity have been obtained by down hole seismic test in BH-3 are shown in Table(1-6) and Fig (1-22). Based on changing seismic velocity some layers physically can be distinguished. From 0 to 7m there is filler material such as cobble, boulder and gravel. From 7 to end of borehole there is seabed materials such as sand, silt, loam shell and gravel that with increasing depth increasing density and velocity. Depth of groundwater during test is about 1m. In Table(1-6) Compression velocity(Vp), Shear velocity(Vs), Elastic modulus(E), Shear modulus(G), Bulk modulus(K) and Poisson ratio(v) are presented.

Table (1-6): Characteristic of compression and shear wave velocity accompany with dynamic parameters in BH-3

Depth(m)	Density(gr/cm3)	Vp(m/sec)	Vs(m/sec)	E(MPa)	G(MPa)	K(MPa)	v
0-1	2	850	480	1167	461	831	0.27
1-2	2	1500	550	1721	605	3693	0.42
2-4	2	1550	600	2033	720	3845	0.41
4-7	2	1600	620	2171	769	4095	0.41
7-9	1.9	1550	550	1641	575	3798	0.43
9-12	1.8	1500	370	723	246	3721	0.47
12-14	1.9	1600	450	1121	385	4351	0.46
14-17	2	1650	540	1680	583	4667	0.44

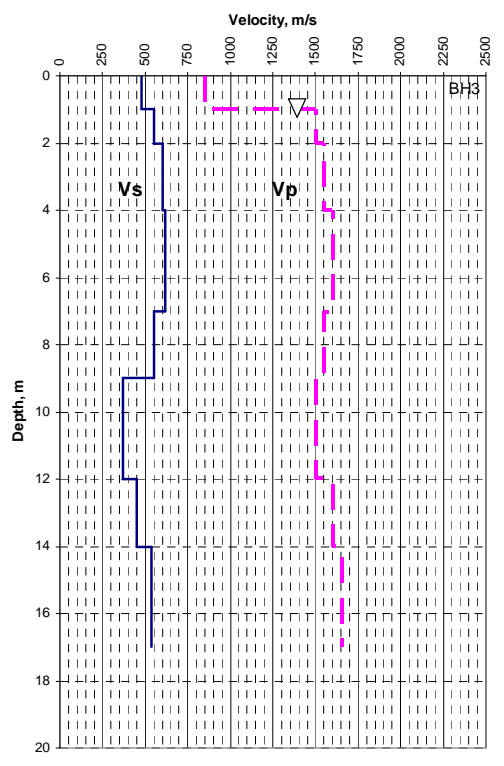


Fig (1-22): The variation of compression and shear velocity verse depth in BH-3 $\,$

6.4 Down hole test in BH-4

Characteristic of compression and shear wave velocity have been obtained by down hole seismic test in BH-4 are shown in Table (1-7) and Fig (1-23). Based on changing seismic velocity some layers physically can be distinguished. From 0 to 5.5m there is filler material such as cobble, boulder and gravel. From 5.5 to end of borehole there is seabed materials such as sand, silt, loam shell and gravel that with increasing depth increasing density and velocity. Depth of groundwater during test is about 1m. In Table (1-7) Compression velocity (Vp), Shear velocity (Vs), Elastic modulus (E), Shear modulus (G), Bulk modulus (K) and Poisson ratio (v) are presented.

Table(1-7). Characteristic of compression and shear wave velocity accompany with dynamic parameters in BH-4

Depth(m)	Density(gr/cm3)	Vp(m/sec)	Vs(m/sec)	E(MPa)	G(MPa)	K(MPa)	v
0-1	2	900	520	1351	541	899	0.25
1-2	2	1500	550	1721	605	3693	0.42
2-4	2	1550	600	2033	720	3845	0.41
4-5.5	2	1500	570	1840	650	3634	0.42
5.5-7	1.9	1500	450	1116	385	3762	0.45
7-10	1.8	1500	370	723	246	3721	0.47
10-14	1.9	1500	430	1022	351	3807	0.46
14-17	1.95	1550	500	1406	488	4035	0.44
17-20	2	1600	600	2042	720	4160	0.42

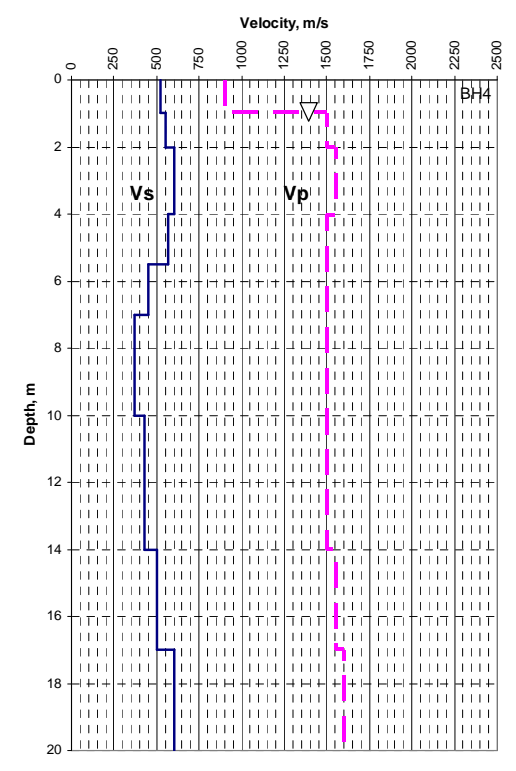


Fig (1-23): The variation of compression and shear velocity verse depth in BH-4

7 Conclusions

Geoseismic tests with two methods of refraction and down hole has been performed in this study. The refraction method has the limitation of blind zone in this study. Because seabed has lower velocity in comparison with the upper man-made soil, seabed layer could not be recognizable by refraction method. Therefore we suggest the refraction method only for surface material. Besides, the down hole seismic test has not this limitation therefore down hole seismic has been selected for site classification. The dynamic properties that have been presented in Tables (1-4) to (1-7) are based on assumption that material is elastic, isotropic and homogenous. These assumptions are suitable only for intact rock rather than other materials as boulder, gravel and sand. There are two code building: Iranian code building No. 2800 Table (1-8) and NEHRP (National Earthquake Hazard Reduction Pogrom) Table (19). In these codes Vs (30) means shear wave velocity to the depth of 30m and is obtained by the following equation:

$$V_{s (30)} = \frac{\sum_{i=1}^{n} T_{i}}{\sum_{i=1}^{n} \frac{T_{i}}{V_{ci}}}$$

Which Ti is thickness of layer I and V_{si} is shear wave velocity. Based on results that obtained in this study, site is classified as type II of Iranian code building and "C" type of NEHRP code Table (1-10).

Table (1-8): Soil profile classification(Iranian Code, Standard No. 2800)

		Standard No. 2000)			
Soil profile type	V _{x (30)} (m/sec)	Description			
1	>750	A)Igneous rock(with coarse and fine grain texture), stiff sedimentary rocks and metamorphic rocks(gneiss and silicate crystal rocks) and conglomerate.			
1	375-750	B)Stiff soils(compacted gravels and sands, very hard clays) with thickness of less than 30m from the bedrock.			
11	375-750	 A)Loose igneous rocks(e.g. tuff), loose sedimentary rocks and laminated metamorphic rocks and in general all loose weathered rocks. 			
п	375-750	B)Stiff soils(compacted gravels and sands, very stiff clays) with thickness of less than 30m from the bed rock.			
Ш	175-375	A)Weathered rocks			
Ш	175-375	B)Rocks of mediocre compaction, gravel and sand layers with mediocre inter- granular links and clays with mediocre stiffness.			
IV	<175	A)Soft deposits with high moisture content due to the high ground water level. B)Soil profile including a minimum of 6m high clay of plasticity index of more than 20 and moisture content of more than 40%.			

Table (1-9): Soil profile classification (NEHRP)

Type	$V_{s(30)}$ (m/sec)
E	<180
D	180-360
С	360-760
В	760-1500
Λ	>1500

Table (1-10): Classification of site based on the downhole tests results

Borehole $V_{z(30)}$ (m/sec) 2800 code NEHRI type					
BH-1	490	II	Ċ		
BH-2	481	11	C		
BII-3	502	п	C		
BII-4	482	II	C		

The downhole geo-seismic test results reveal that the shear wave velocity within the surface fill layer is higher than its counterpart in sandy layer of the natural surface. The depth of the fill varies between 5 and 8m. With respect to the fact that the compressive wave velocity of water is about 1500 to 1600m/s, it might be higher than the velocity in the soil material, thus the calculated modules are higher than the dry materials' modules. Moreover the calculated modules by the geo-physical methods gain a value of several times higher than the modules of laboratory dynamic/cyclic test results, because the strain limit within the geo-physical methods are much smaller than the strain limits in laboratory tests.



Fig (1-24): The used seismograph, ABEM RAS 24 apparatus



Fig (1-25): A photo of used electrical resistivity device



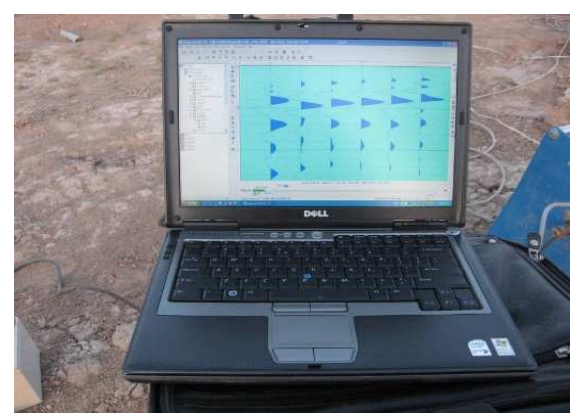
Fig (1-26): Equipments used in electrical resistivity tests



Fig (1-27): A picture of the used geophones in seismic tests



Fig (1-28): A picture of the used down hole geophones



Fig(1-29). A sample of graphs obtained from the tests

8 Introduction

In this study 22 electrical resistivity sounding with maximum current source length 100m have been taken. Equipments that have been used in this field work are as following:

- -Resistivity meter.
- -Battery (12volt DC).
- -Global Positioning System(GPS).
- -Notebook computer.
- -Stainless steel electrode.
- -Bras electrode.
- -Multimeter.
- -Other accessory, cable, render, wire and etc.

8.1 Theory of electrical resistivity test

In this method the current source causes a direct current i to flow through the earth, entering at electrode C1, and leaving from electrode C2. The potential difference will be measured between P1 and P2 electrodes. The lines of current that flow through the earth are 3-D. Their distribution can be computed theoretically although it may be quite complicated, especially for complex geology. The lines of flow current are always perpendicular to surface along which the potential is constant, the later being referred to as equipotential. The relationship is illustrated by the cross section in Fig(2-1). The potential difference(or voltage) impressed across electrodes C1 and C2 is

distributed along the space between them. In a homogeneous medium, the potential with respect to C1 along a vertical plane cutting the surface at midway between C1 and C2, will be half as great as its value at C2. The apparent resistivity can be calculated by: $\rho a = K.\Delta V \, / \, I$

Where K is geometrical factor and depends on relative distance between current and potential electrodes. The relationship between the apparent resistivity and real resistivity is a complex relation. To determine the true subsurface resistivity, an inversion of the measured apparent resistivity values using a computer program must be carried out. The measured apparent resistivity values are normally plotted on a log-log chart.

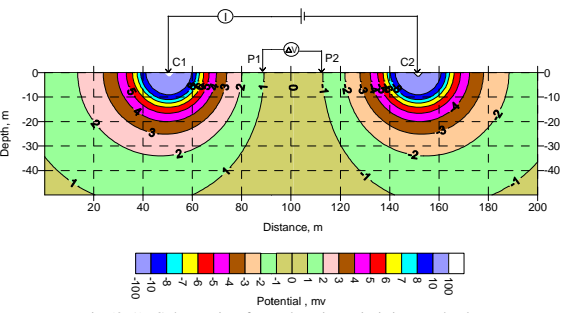


Fig (2-1): Schematic of geoelectric resistivity method

8.2 Values of electrical resistivity of different materials

Electrical resistivity of rocks depended on type of minerals. The important factors in electrical special resistivity are fellowmen:

- -The volume of profuse and fracture
- -The relation between profuse and tracks
- -The volume of profuse that filled with water
- -Conductivity of water exists in rock
- -Type of mineral

Therefore special electrical resistivity of layers depended on geology condition. Special electrical resistivity some materials are presented in Table(2-1).

Table (2-1): Special electrical resistivity of some materials

Rock and water type	Specific electrical resistivity(Ohm.m)
Sea water	0.2
Alluvial water	10-100
Natural spring water	50-100
Dry gravel and sand	1000-10000
Saturated gravel and sand by fresh water	50-500
Saturated gravel and sand by salt water	0.5-5
Clay	2-20
Marl	20-100
Lime	300-1000
Argillite sand stone	50-100
Quartzite sand stone	300-10000
Lava	300-10000
Graphitic schist	0.5-5
Argillite schist	100-300
Fresh schist	300-3000
Gneiss weathered granite	100-1000
Gneiss fresh granite	1000-10000

8.3 Electrical resistivity results

In this study 22 sounding point along 6 profile(line or section) with Wenner–Schulmberger, four electrodes and

length current 200m have been taken. The coordinate of sounding points are presented in Table (2-2). The location maps of these points are shown in Fig (2-2).

Table (2-2): Coordinate of electrical resistivity sounding

Soundage	X	Y
s1	615972	3066800
s2	616003	3066837
s3	616042	3066866
s4	616079	3066896
s5	616117	3066933
s6	616151	3066966
s7	616161	3066968
s8	616130	3066936
s9	616091	3066895
s10	616061	3066861
s11	616018	3066830
s12	615984	3066796
s13	615913	3066939
s14	615949	3066930
s15	615993	3066917
s16	615989	3066905
s17	615940	3066917
s18	615899	3066929
s19	616069	3066803
s20	616100	3066756
s21	616114	3066764
s22	616098	3066811

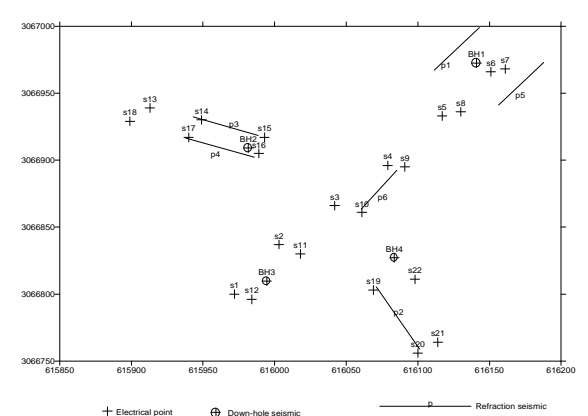


Fig (2-2): Location of electrical resistivity sounding points

8.3.1 Profile A-A'

This section included 6 soundage S1, S2, S3, S4, S5 and S6 with Schulmberger array and max current length(AB) 200m located on main branch. Apparent resistivity or row data are shown in Fig(2-3). The true(interpreted) section has been shown in Fig(2-4). We can see soundage S1 and S2 has low resistivity than others since sea water inject rock material. Some parts such as S4, S5 and S6 the width of filler material more than other parts therefore this area has more resistivity. In this section soundage S6 has more thickness layer with resistivity more than 10ohm.m, which it seems by increasing distance from cost material is become finer.

8.3.2. Profile B-B'

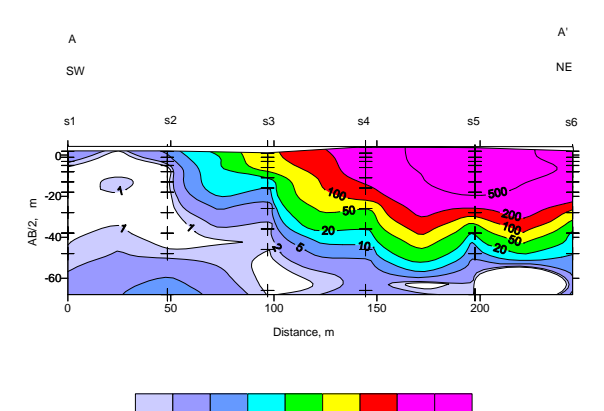
This profile is included 6 soundage S7, S8, S9, S10, S11 and S12 with Schulmberger array and maximum current length 200m located on main branch. Apparent resistivity or raw data are shown in Fig (2-5). The real profile(interpreted) has been shown in Fig (2-6). We can see soundage S11 has low resistivity than others, since sea water is penetrated to soil layers and soil type is fine grained. Some parts such as S7, S8 and S9 the thickness of man-made soil is more than other parts, therefore this area has more resistivity. In this profile soundage S7 has more thickness layer with resistivity more than 10ohm.m, that it seems by increasing distance from cost material is become finer.

8.3.3 Profile C-C'

This profile is included 4 soundage S13, S14, S15, and S4 with Schulmberger array and maximum current length 200 m. Apparent resistivity or raw data are shown in Fig(2-7). The real profile has been shown in Fig(2-8). We can see soundage S13 and S14 has low resistivity than others since sea water is penetrated to soil layers. Some parts such as S4 the thickness of man-made soil is more than other parts, therefore this area has more resistivity.

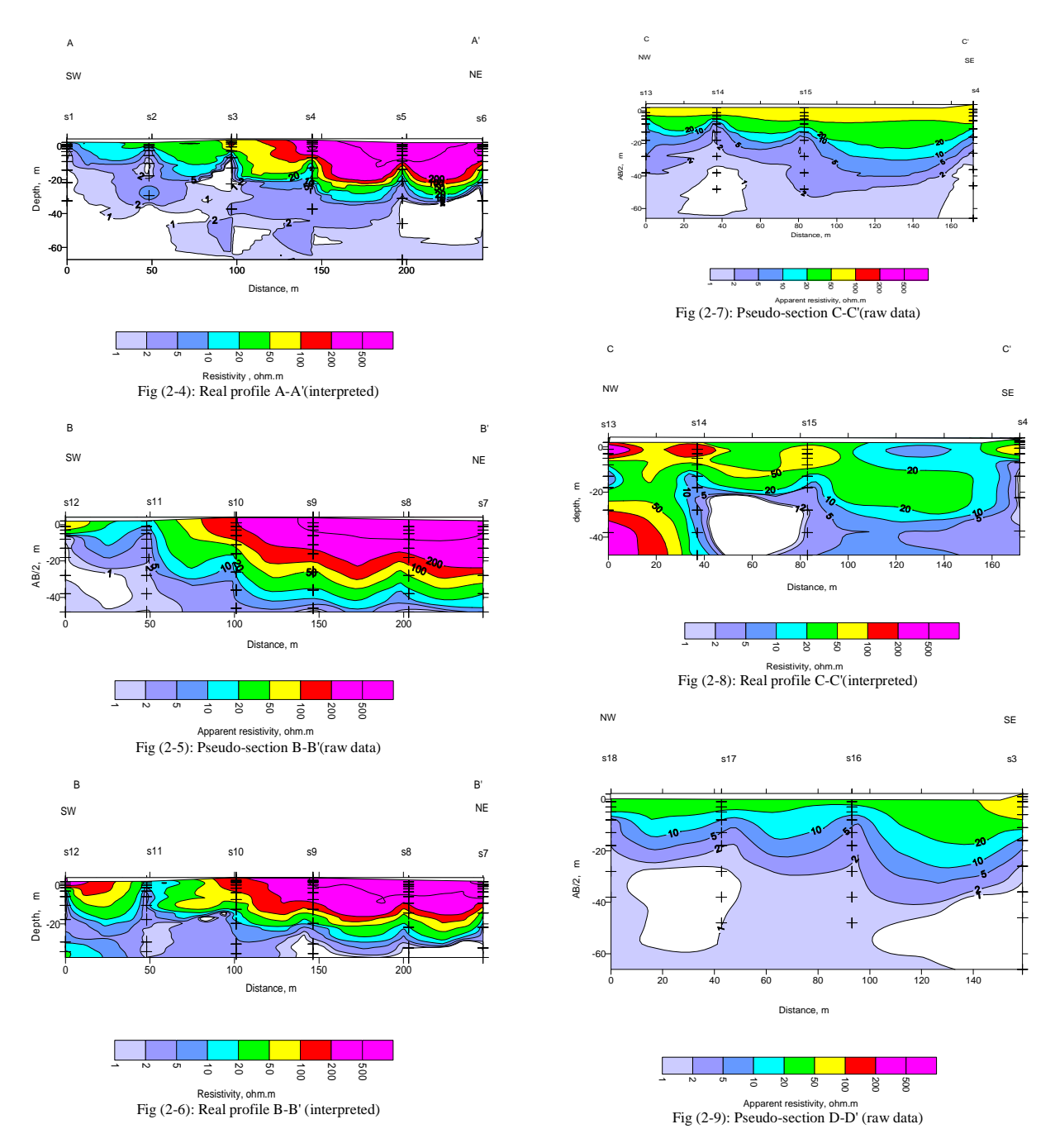
8.3.4. Profile D-D'

This profile is included 4 soundages S18, S17, S16 and S3 with Schulmberger array and maximum current length 200m. Apparent resistivity or raw data are shown in Fig(2-9). The real profile has been shown in Fig(2-10). We can see soundage S18 and S17 has low resistivity than others since sea water is penetrated to soil layers. Some parts such as S3 the thickness of man-made soil is more than other parts, therefore this area has more resistivity.



Apparent resistivity , ohm.m Fig (2-3): Pseudo-section A-A'(raw data)

0



8.3.5 Profile E-E'

This profile is included 3 soundages S9, S22 and S21 with Schulmberger array and maximum current length 200m. Apparent resistivity or raw data are shown in Fig(2-11). The real profile has been shown in Fig(2-12). We can see soundage S9 and S22 has low resistivity than others due to sea water is penetrated to soil layers. Some parts such as S21 the thickness of man-made soil is more than other parts, therefore this area has more resistivity.

8.3.6. Profile F-F'

This profile included 3 soundage S10, S19 and S20 with Schulmberger array and maximum current length 200m. Apparent resistivity or raw data are shown in Fig(2-13). The real profile has been shown in Fig(2-14). We can see soundage S19 and S20 has low resistivity than others since sea water is penetrated to soil layers and maybe finer material. Some parts such as S20 the thickness of manmade soil more than other parts, therefore this area has more resistivity.

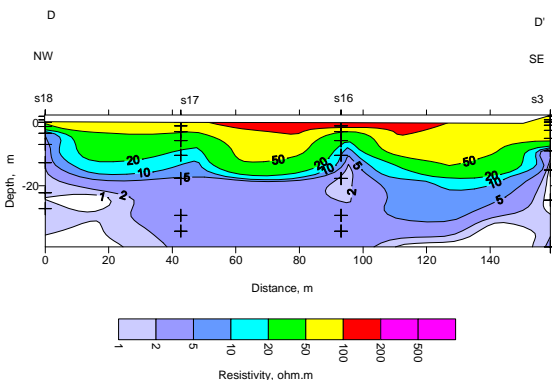


Fig (2-10): Real profile D-D'(interpreted)

9. Conclusions

It can be inferred from the derived results of the geophysical investigations that the electrical resistivity at the 'fill' zone (which has higher extents of pores) is less than the other zones. Within the natural surface layers, the electrical resistivity value varies between 1 to 500ohm.m. The higher amounts of resistant is a sign of existence of the granular layers, while the lower amounts stand for the existence of fines. The electrical resistance gains its lowest value at the location of soundages S22, S21, S20, S19, and S1. Therefore, specific consideration shall be staged at the latter locations.

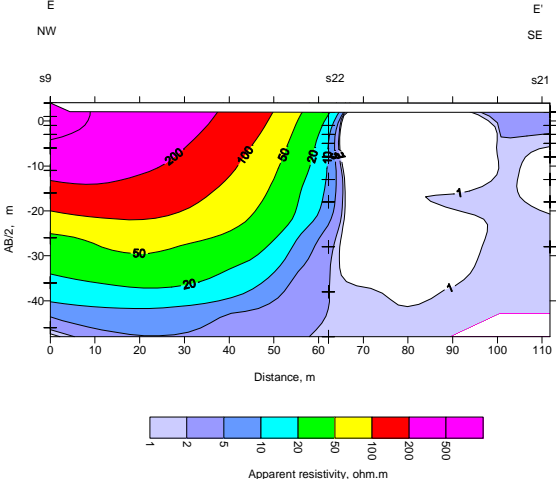


Fig (2-11): Pseudo-section E-E' (raw data)

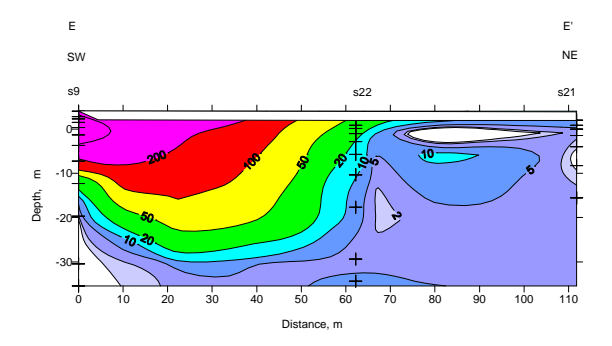
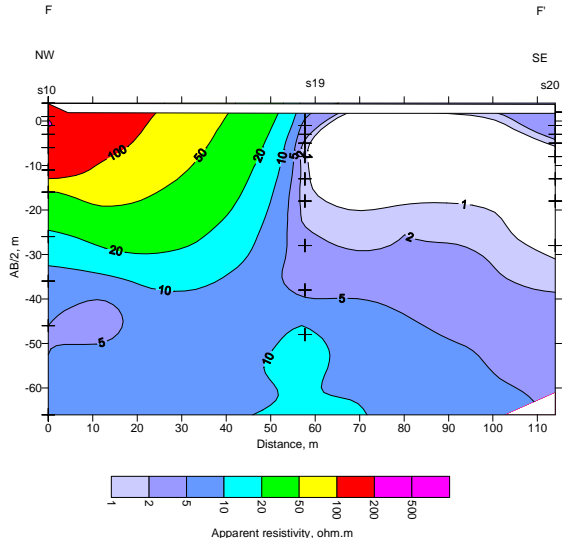
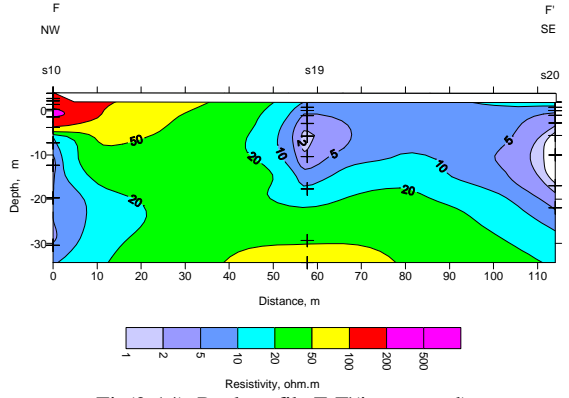




Fig (2-12): Real profile E-E'(interpreted)



Apparent resistivity, ohm.m Fig (2-13): Pseudo-section F-F'(raw data)



Fig(2-14). Real profile F-F'(interpreted)

References

1- Taher Rajaee, Vahid Nourani, Mohammad Zounemat-Kermani and Ozgur Kisi, 2011. River Suspended Sediment Load Prediction: Application of ANN and Wavelet Conjunction Model. Journal of Hydrologic

- Engineering, ASCE, Volume 16, No. 8, Agust 1, 613-627.
- 2- Rajaee, T., Mirbagheri, S.A., Nourani, V., Alikhani, A., 2010. Prediction of daily suspended sediment load using wavelet and neuro-fuzzy combined model. International Journal of Environmental Science and Technology (IJEST), 7 (1), 93-110, Winter.
- 3- Bathurst, R.J., Keshavarz, A., Zarnani, S. and Take, A. (2007). A simple displacement model for response analysis of EPS geofoam seismic buffers. Soil Dynamics and Earthquake Engineering, Vol. 27: 344-353.
- 4- Jahanandish, M., and Keshavarz, A. (2005). Seismic Bearing Capacity of Foundations on Reinforced Soil Slopes, Geotextiles and Geomembrains, Vol. 23 (1): 1-25.
- 5- Jahanandish, M., and Keshavarz, A. (2004). Stability of Axially Symmetric Slopes in Soil Engineering, Proceedings of International Conference on Geotechnical Engineering, Beirut, 19-22 May 2004
- 6- Jahanandish, M., and Keshavarz, A. (2004). Evaluation of Critical Load Distribution of Foundations on Slopes by the Zero Extension Line Method. Proceedings of the 4th International Conference on LANDSLIDES, SLOPE STABILITY & THE SAFETY OF INFRASTRUCTURES, Kuala Lumpur, Malaysia, 2004
- 7- M. Gharouni e nik, Designing an Underground Lead and Zink Mine Using In-Situ Initial State of Stresses, Rock Stress and Earthquakes - Xie (ed.), Taylor & Francis Group, London, ISBN 978-0-415-60165-8.2010.
- 8- Ali Mansourkhaki, A.Arabani, "Rational analysis of asphalt corrugation at Intersections" Journal of Engineering Volume 11 No2, Calcutta, India, April 2001.
- Ali Mansourkhaki. M.Ameri. M.Arabani, "Determination of cohesion and friction angle of Asphalt Concrete based on Uniaxial and indirect tensile test. "Int, J. Engng. IUST, 12 No2 (2001).
- 10- Mansour Khaki, Ali. and Reza Moayedfar, "The development of the composed probability model to estimate the rate of household trip production (Case study of Karaj city)", International Journal of Civil Engineering (IJCE), Vol. 2, No. 2, pp. 72-77, June 2004
- 11- Ali Mansourkhaki , Sahryar Afandizadeh, Reza Moayedfar, "Developing The Composed Probability Model to Predict Household Trip Production", Transport, Vilnius Gediminas Technical University, Lithuanian Academy of Science, 2009 24(1).
- 12- Ali Mansourkhaki ,M.Hosseaini,A.Shariat,(2003) Evaluating the efficiency of urban Transportation System in the aftermath of Earthquake in Large populated Cities,International Journal of Engineering Science,Iran University of science and Technology.
- 13- Mansour khaki, A., shariat mohymany, A. and S.H. sadati "Determining the Hydrologic Index for prioritization of the strengthening the components of transportation Network against flood (Golestan province case study)", Journal of Applied sciences Research, RJAS, 5(10): 1714-1720, 2009.

- 14- Mansour khaki, A., shariat mohymany, A. and S.H. sadati, "Development an Accessibitiyy approach to rank the transportation Network components during the occurrence of flood crisis (Golestan province case study) ", Australian Journal of Basic and Applied Sciences, 2229 AJBAS, 2010.
- 15- Ahmad Adib, Alireza Ashofteh, Geotechnical & foundation engineering studies of aditional structures of phase 12 of south pars gas(tombak region), Journal of Basic and Applied Scientific Research(JBASR), ISSN2090-4304, September 2013, Special Issue(1), Vol 3, No 9, Pages: 662-684, SP-129



Eng.Alireza Ashofteh Was born in iran on january 1982. He received the M.Sc degree in mining engineering. He is a member of young researchers and elite club, islamic azad university north tehran branch, tehran, iran, st_a_ashofteh@azad.ac.ir



Eng.Sharareh Hajali Was born in iran on 1984. She received the M.Sc degree in geology tectonics, islamic azad university north tehran branch, tehran, iran, sh.ha_7@yahoo.com